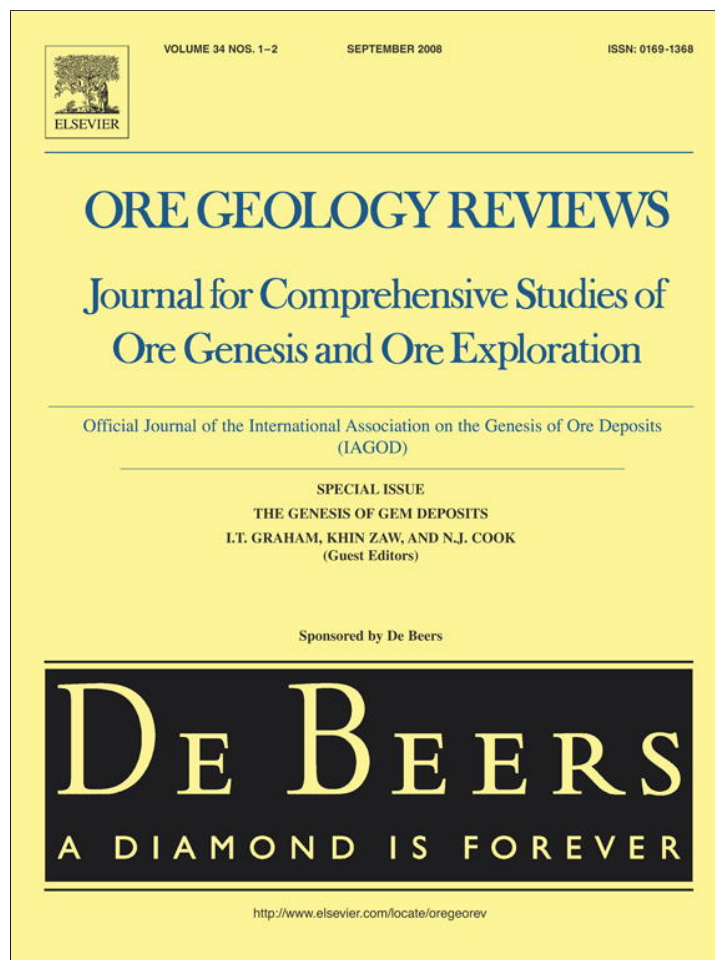


Provided for non-commercial research and education use.
Not for reproduction, distribution or commercial use.



This article appeared in a journal published by Elsevier. The attached copy is furnished to the author for internal non-commercial research and education use, including for instruction at the authors institution and sharing with colleagues.

Other uses, including reproduction and distribution, or selling or licensing copies, or posting to personal, institutional or third party websites are prohibited.

In most cases authors are permitted to post their version of the article (e.g. in Word or Tex form) to their personal website or institutional repository. Authors requiring further information regarding Elsevier's archiving and manuscript policies are encouraged to visit:

<http://www.elsevier.com/copyright>



Contents lists available at ScienceDirect

Ore Geology Reviews

journal homepage: www.elsevier.com/locate/oregeorev

Ultrahigh pressure macro diamonds from Copeton (New South Wales, Australia), based on Raman spectroscopy of inclusions

L.M. Barron^{a,*}, B.J. Barron^b, T.P. Mernagh^c, W.D. Birch^d^a Geological Survey, New South Wales Department of Primary Industries PO BOX 344, Hunter Region Mail Centre, NSW 2310, Australia^b 7 Fairview Avenue, St. Ives, NSW, 2075, Australia^c Geoscience Australia, GPO Box 378, Canberra ACT 2601, Australia^d Museum Victoria, GPO Box 666 Melbourne, Victoria 3001, Australia

ARTICLE INFO

Article history:

Received 15 July 2006

Accepted 14 July 2007

Available online 21 May 2008

Keywords:

Diamond

Raman

Ultrahigh pressure

Coesite

Omphacite

Diopside

Grossular

Olivine

Carbonate

Strain birefringence

ABSTRACT

Mining of Cenozoic alluvial deposits at Copeton and Bingara (Eastern Australia) has produced two million macrodiamonds (0.25 ct median size). Raman spectroscopy is used to identify included minerals within uncut Copeton diamonds, with sealed chamber remnant pressures of 31.7 to 35.6 kbar for coesite, 13.6 and 22.7 kbar for clinopyroxene, and 7.6 kbar for grossular garnet. Assuming elastic behaviour, these values generate inclusion entrapment PT loci which intersect, restricting diamond formation conditions: from 250 °C, 43 kbar to 800 °C, 52 kbar. Larger than error (± 100 °C and ± 4 kbar), this range shows a systematic variation in inclusion composition with diamond zoning and N properties. Published research shows 1) Copeton and Bingara diamonds are unique, and 2) modern alluvium in the Bingara district carries mantle-formed garnet, captured by post-tectonic alkali basalt from an extensive diamondiferous ultrahigh pressure (UHP) terrane that stalled at depth because it is dominated by mafic eclogite. The combined Raman and geological results indicate two sets of subduction UHP diamond formation conditions/protolith are required, firstly cooler oceanic slab and secondly including higher temperature continental crust. The Copeton and Bingara stones are UHP macrodiamonds, and Carboniferous $^{40}\text{Ar}/^{39}\text{Ar}$ age dates on clinopyroxene inclusions should be interpreted as ages of crystallisation, representing the termination of subduction. The characteristic features of ruptured inclusions and etched percussion marks on Copeton and Bingara diamond indicate volcanic delivery to the earth's surface. Alluvial deposits elsewhere in Eastern Australia may carry similar diamond along with diamond of different origin.

Crown Copyright © 2008 Published by Elsevier B.V. All rights reserved.

1. Introduction

About 500,000 ct of macrodiamond were produced (Fig. 1) from paleoalluvial deposits buried under intraplate Cenozoic basalt in Eastern Australia (MacNevin, 1977). About 94% of the total production was from a 400 km² area at Copeton (150° 55' longitude E, -29° 57' latitude S), and another 4% from a similar sized area about 65 km to the west (Bingara). Both areas are part of the New England Fold Belt (NEFB), which is faulted against the older Tasman Fold Belt (TFB) of New South Wales (NSW). The NEFB is a terrane assembled by accretion due to Phanerozoic subduction (Scheibner, 1998), more than 1500 km from the nearest craton (the 1.4 Ga North Australian Craton). The two fold belts developed separately until the NEFB docked against the TFB along the 1200 km long Peel – Great Moreton – Yarrol Fault system during Late Permo-Triassic westerly subduction, with episodic

subduction continuing on the eastern margin of the NEFB through to the end of the Mesozoic.

Research on Copeton and Bingara diamonds (MacNevin, 1977; Sobolev, 1984; O'Reilly, 1989; Barron et al., 1996; Meyer et al., 1997; Davies, 1998; Griffin et al., 2000; Davies et al., 2002, 2003; Hollis, 2003) shows that most have rounded shapes with dodecahedral and tetrahedral morphologies, either completely unzoned (about 50% of diamonds), or strongly zoned under growth conditions of high strain deformation and brecciation. Such rounded shapes are typical of resorbed diamonds, the loss taking place during deep storage (Robinson, 1980; Robinson et al., 1989), and/or magmatic delivery to the earth's surface (experimental, Fedortchouk et al., 2005; Khokhrayakov and Pal'yanov, 2007). Resorption truncation of zoning is visible on many uncut Copeton and Bingara stones and they have a relatively small modal size (0.25 ct, MacNevin 1977). Davies (1998) and Griffin et al. (2000) estimated that more than 85% of Copeton and Bingara diamonds have lost >50% volume by resorption, although a recent experimental study (Khokhrayakov and Pal'yanov, 2007) indicates the same shapes could be reached with much less resorption (20 to 25%). In keeping with these lower degrees of resorption, virtual addition of diamond layers to Copeton stone 96.10 (Fig.

* Corresponding author. Present address: Australian Museum, 6 College St, Sydney, NSW 2010, Australia. Tel./fax: +61 2 94495839.

E-mail address: barronjandl@optusnet.com.au (L.M. Barron).

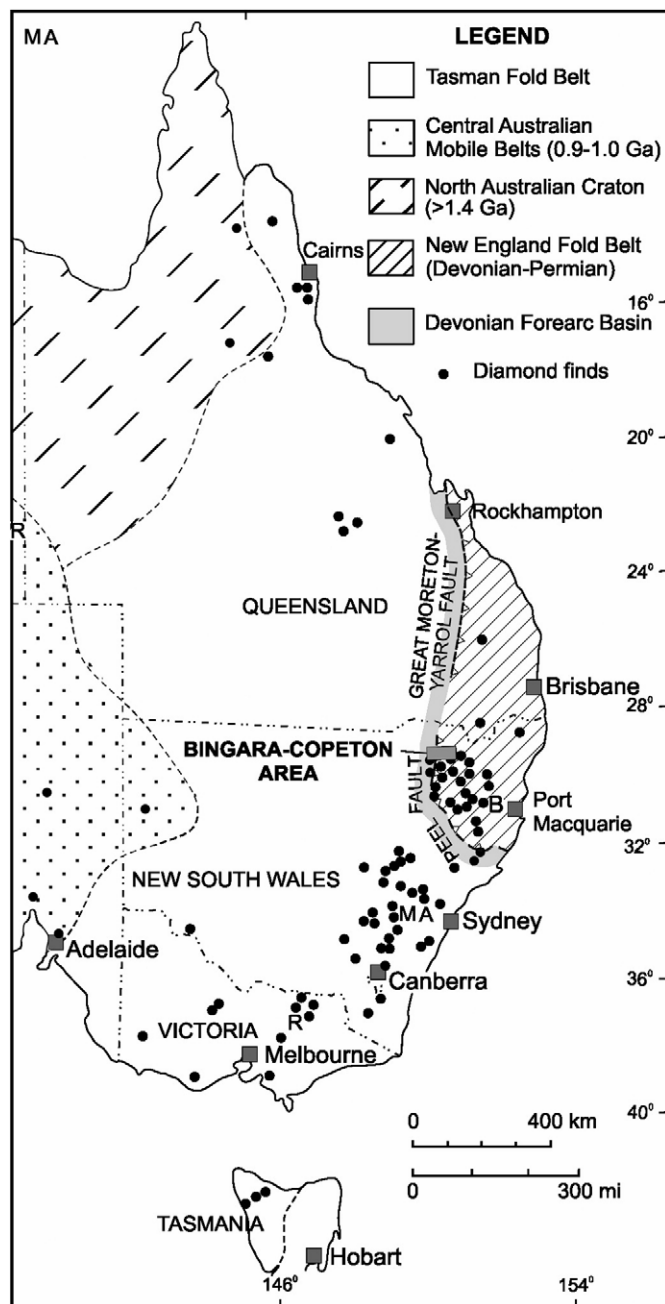


Fig. 1. Locality map of eastern Australia, showing major geological features and occurrences of alluvial diamond, including New South Wales (Copeton, Bingara, Brick Clay Creek—left of B, Mount Airly—above A of MA), and Rutherglen (above R, Victoria).

5 in Barron et al., 1996) would cause the perfectly smooth large euhedral indents to enlarge and meet with only 26% addition. According to Davies et al. (2003), the Bingara diamonds show little evidence of alluvial transport damage, although a few percent of diamonds have green or brown radiation spots. Based on our observations of 2000 stones, Copeton diamonds show a comparable alluvial history.

A suite of unusual inclusions in Copeton and Bingara diamonds (grossular, omphacite, diopside, olivine, calcite, melillite, titanite, amphibole, scapolite, and sulphides) was identified variously as rodingitic/calc-silicate/eclogitic (Sobolev, 1984; Meyer et al., 1997; Milledge et al., 1998; Davies, 1998; Griffin et al., 2000; Davies et al., 2002, 2003). Davies (1998) and Davies et al. (2003) determined that a minor majoritic component was present in some garnet inclusions in Bingara diamonds, so that elevated pressures of formation consider-

ably above 20 kbar were likely. Davies (1998), estimated a PT locus (30 kbar, 790 °C to 60 kbar, 840 °C) passing through diamond formation conditions using the compositions of separate grossular and clinopyroxene inclusions in different Bingara diamonds, based on Krogh's (1988) technique. Age dates on the diamonds include Carboniferous $^{40}\text{Ar}/^{39}\text{Ar}$ dates on clinopyroxene inclusions (Burgess et al., 1998 and Pearson et al., 1998, Copeton diamond; Davies 1998, Bingara diamond) and Mesozoic Pb/U date on titanite (Davies et al., 2002, Bingara diamond).

In central NSW, 100 km WNW of Mount Airly, 20,000 diamonds were recovered from alluvial deposits derived through erosion of Cenozoic palaeoalluvial deposits (MacNevin, 1977). Based on isotope, nitrogen, and inclusion studies in a parcel of more than 500 stones (Davies, 1998; Griffin et al., 2000; Davies et al., 2002, 2003), about 80% were formed in Proterozoic mantle, but such diamonds have not been found at Copeton or Bingara. There has been no comparable research on diamond from the remaining alluvial and palaeoalluvial occurrences in NSW or Victoria, but they demonstrate local variation in diamond shapes, sizes and nitrogen properties (MacNevin, 1977; Birch and Barron, 1997; Sutherland and Barron, 2003).

A compilation of nitrogen content and degree of B aggregation in diamond (Taylor et al., 1990; Meyer et al., 1997; Davies, 1998; Davies et al., 2002, 2003) indicates that two groups of diamond are found at Copeton and Bingara: the zoned group of white diamonds with low N (<500 ppm, low to moderate %B), and the unzoned group of mostly yellow diamonds with high N (500 to 3000 ppm, moderate to high %B). For diamonds from elsewhere in NSW, an additional three groups are present: Davies et al. (2002) reported one group with (moderate N, high %B) and a second with (high N, low %B), whereas Sutherland and Barron (2003) reported a small third group with high N but virtually nil B aggregation at Brick Clay Creek, Walcha (NSW).

Three source models have been proposed for the Copeton and Bingara diamonds (Sobolev, 1984; Sutherland et al., 1985; O'Reilly, 1989; Taylor et al., 1990; Sutherland et al., 1994; Barron et al., 1996; Burgess et al., 1998; Davies, 1998; Griffin et al., 2000; Davies et al., 2002, 2003; Sutherland and Barron, 2003; Barron et al., 2005): 1) cratonic diamonds have been glacially transported from Antarctica (Carboniferous dates interpreted as emplacement); 2) diamonds are from metastably preserved volumes of cool lithosphere (ancient or Phanerozoic); and 3) diamonds formed during subduction (i.e., cold subduction; Robinson, 1978), either ancient or Phanerozoic. Some models proposed volcanic delivery of the diamonds to the earth's surface (by kimberlitic/lamproitic or alkali basaltic magmas), supported by the presence of magmatically etched percussion marks on some Copeton and Bingara diamonds (Meyer et al., 1997; Hollis, 2003).

Most Cenozoic diamond-bearing alluvial deposits lack indicator minerals, but trace garnet is recorded in some (MacNevin, 1977). However near Bingara, Barron et al. (2005) reported significant garnet abundance (with a high proportion of mantle garnet) recovered from modern stream sediment samples across a 200 km² area, and concluded that this garnet was derived from a diamondiferous UHP terrane dominated by mafic eclogite. This UHP terrane, assembled by termination of Carboniferous and Mesozoic subduction, is extensive but does not outcrop, so it was trapped at depth after partial decompression produced crystallographically-oriented exsolution textures in some garnet and clinopyroxene. The alluvial garnet compositions show local variation around Mesozoic alkali basaltic intrusions which must have intersected the UHP terrane at depth. Geological evidence (Helmstaedt and Doig, 1975; Xu et al., 2005) suggests that subducted UHP parcels of rock at depths in the crust can retain their relatively low temperatures for more than 70 MY, with implications for survival of UHP diamond.

Raman spectroscopy is used to identify mineral inclusions in diamonds from known localities and to estimate their compositions and remnant pressures. These results are combined with the diamond-

Table 1
Definition of symbols and terms used

P, T	Pressure (bars), temperature (°C)
P_f, T_f	P and T of formation of diamond
P_c	Confining pressure on an inclusion in diamond at general P - T
P_r	Remnant pressure: P_c when diamond is at the conditions of the Earth's surface (0 bars, 0 °C).
P_d	Pressure difference between P_c and P for a general P - T , representing on diamond from inclusion
A	Coefficient of isobaric thermal expansion
B	Coefficient of isothermal compressibility
A_h, A_d, A_i	A for host; diamond; included mineral

inclusion model of Barron (2005) to estimate the diamond formation conditions.

2. Technique

2.1. Selection of suitable diamond

About 3000 diamonds from known localities in eastern Australia were examined using binocular and petrological microscopes. Most were Copeton and Bingara diamonds. A small number of diamonds were examined from other Cenozoic palaeoalluvial deposits within eastern Australia, namely Mount Airly (NSW, 150° 02' E, 33° 05' S), and Eldorado and Rutherglen in Victoria (Great Southern Deep lead, Victoria, 146° 28' E, 36° 03' S). There are reports of diamond occurring in alkali basaltic breccia, and diamonds from two such localities were examined—Brick Clay Creek (151° 27.36' E, 31° 2.9' S; Sutherland and Barron, 2003), and a Copeton mine called Wonderland (MacNevin, 1977). Diamonds showing strain birefringence were selected for more careful examination. Inclusions were found in 110 diamonds, mainly from Copeton (42 yellow and 47 white stones). The inclusions were ranked based on 1) whether the strain birefringence in the diamond was inclusion-related; 2) visibility of inclusion under low and high magnification; and 3) whether this visibility was influenced by features on the outer surface of the diamond. This ranking was used to select the best diamonds (52) for analysis by Raman spectroscopy, including 21 yellow and 20 white stones from Copeton.

2.2. Raman spectroscopy

Raman spectroscopy has been widely used to identify minerals and their approximate compositions. The Raman technique is especially useful because it is non-destructive and can be applied to inclusions in-situ. Raman spectroscopy has been used on inclusions in diamonds—see Liu et al. (1990), Izraeli et al. (1999), and Sobolev et al. (2000) for variations on the technique. The Raman spectrum of a mineral is sensitive to pressure, and calibrated factors of the pressure shift are published for many minerals. In the present work the following Raman reference data is used for (mineral, reference peak, pressure conversion factor, reference): (coesite, 520.6 cm⁻¹, 0.29 cm⁻¹/GPa, Hemley, 1987) and (diamond, 1332 cm⁻¹, 2.64 cm⁻¹/GPa; Tardieu et al., 1990).

Raman spectra were recorded on a Dilor SuperLabram spectrometer equipped with a holographic notch filter, 600 and 1800 g/mm gratings, and a liquid nitrogen-cooled, 2000×450 pixel CCD detector. The diamonds and their inclusions were illuminated with 514.5 nm laser excitation from a Melles Griot 543 argon ion laser, using 5 mW power at the samples. A 50X ULWD Olympus microscope objective (numerical aperture of 0.55) was used to focus the laser beam and collect the scattered light. The focused laser spot on the sample was approximately 2 μm in diameter with a thickness of the focal plane of about 5 μm. Raman shifts were accurate to ±0.1 cm⁻¹ as determined by plasma and neon emission lines, and the spectral resolution was set at 2 cm⁻¹ with a slit width of 100 μm. The peak position of a well defined

peak in the spectra was demonstrably reproducible to 0.1 cm⁻¹, for both low (0 kbar) and high (35 kbar) remnant pressure values. Barron et al. (2008) provide details about the exact techniques and rationale used to generate the data herein.

2.3. Theory: diamond formation conditions from remnant pressure

The volume behaviour of inclusions in other minerals has been modelled, assuming elastic behaviour, by Smith (1953), Rosenfeld and Chase (1961), Harris et al. (1970), Adams et al. (1975), Cohen and Rosenfeld (1979), Liu et al. (1990), Zhang (1998), Izraeli et al. (1999), and Sobolev et al. (2000). Recently, Barron (2005) showed that all topological aspects of the diamond/inclusion relation were preserved in a simple linear model called the Pressure Preservation Index model (PPI). Furthermore the PPI model had ±1% accuracy up to 55 kbar, 1300 °C compared to published fully corrected results. The isovolume locus is given by

$$P/T = (A_d - A_i)/(B_d - B_i), \quad (1)$$

where A is the isobaric coefficient of thermal expansion, and B is the isothermal compressibility for host diamond (d) and inclusion (i) (Table 1). The isovolume locus passes through the (0 °C, 0 kbar) origin representing conditions at the Earth's surface, and has a positive slope according to Eq. (1), see Table 2 for sample values of minerals found as inclusions in Copeton and Bingara diamonds.

The PPI model shows there are three different topological inclusion groups (heritage, mixed, negative), based on whether the isovolume locus of a mineral passes below, through or above the pressure range of cratonic diamond formation conditions, respectively. Heritage group inclusions generate high positive remnant pressure, negative group inclusions typically completely decompress, whereas mixed group inclusions generate small positive or negative remnant pressure. The isovolume locus of a mineral species is relatively insensitive to extreme variations in solid solution chemistry (see Adams et al., 1975), so a mineral species can be reliably assigned to a particular inclusion group.

Table 2

Minerals reported as inclusions in Copeton and Bingara diamonds, inclusion group (diamond host), calibration data (volume coefficients: A =isobaric thermal expansion per °C, B =isothermal compressibility per bar, ×10⁶ means table value is one million times the coefficient), and some predicted values from the PPI model (Barron, 2005) for estimated formation conditions of Copeton diamond

Inclusion group	Mineral (abbreviation)	A	B	Source	Isovolume at 1000 °C	PPI model P_r (kbar) for formation conditions	
		×10 ⁶	×10 ⁶	A, B	P kbar	250 °C, 43 kbar	800 °C, 52 kbar
Heritage	Diamond	0.708	0.238	2, 2			
	Graphite (Gra)	8.4	2.8	5, 15	3.0	39	45
	Coesite (Coe)	5.43	1.002	13, 9	6.2	32	36
	Calcite (Cal)	38	1.49	6, 17	29.7	30	23
	Melilite (Mel)	24.9	0.996	1, 1	31.9	27	20
Mixed P_r	Tremolite (Tr)	31.3	1.176	14, 4	32.6	28	21
	Dolomite (Dol)	37.4	1.22	12, 10	37.4	27	18
	Scapolite (Sca)	51.8	1.53	19, 20	39.5	28	17
	Titanite (Ttn)	25	0.76	8, 8	46.5	22	10
	Grossular (Grs)	25	0.72	13, 7	50.4	20	8
	Diopside (Di)	33.4	0.886	16, 16	50.5	22	9
	Forsterite (Fo)	26.4	0.73	6, 11	52.2	20	7
Negative	Anatase	27.2	0.559	18, 3	82.6	13	-8

Abbreviations for minerals are after Kretz (1983) and Spear (1993). Data source numbers: 1 Berman (1988); 2 Berman (1994); 3 Arlt et al., 2000; 4 Comodi et al., 1997; 5 ESPI website (2004); 6 Fei (1995); 7 Hazen and Finger (1976a,b); 8 Holland and Powell (1985); 9 Levien and Prewitt (1981); 10 Martens et al. (1982); 11 Olinger (1977); 12 Reeder and Markgraf (1986); 13 Fei et al. (1990); 14 Sueno et al. (1973); 15 Tang et al. (2000); 16 Wechsler and Prewitt (1984); 17 Zhang and Reeder (1999); 18 Horn et al. (1972); 19 Baker (1994); 20 Bass (1995).

Table 3
Details of important diamonds, mostly with Raman spectroscopy identification of inclusion and remnant pressure determinations

Diamond	Source/mine	Size mm/ shape	Colour	Inclusion/size in μm /shape	Influence on diamond	Raman peak cm^{-1}	P_r kbar/ method Internal (I) or External (E)
96.22	Copeton/ Star of South	3/rounded	White	Coesite/100/equant cloudy brown. Sixteen other inclusions that failed to give a raman response	Cracks reaching surface, strong birefringence	526.2, 527.2	19.3, 22.8/I
G1*	Mount Airly/ Whites	3/elongate rounded	White	Clinopyroxene /30/equant	No cracks, weak birefringence	670, 1010	4.2/E
JB05*	Copeton/ Wonderland	Long 4 mm/ ellipsoid	Pale yellow	Coesite/300/thin wedged plate	No cracks, strong birefringence	529.8	31.7/I
JB16*	Copeton/ Wonderland	Flat 3.5 mm/ curved	Pale yellow	Coesite/570/ gently Z-kinked plate	No cracks, strong birefringence	530.6	34.5/I
L001*	Copeton/ Staggy Creek	Flat 5 mm/ curved	Pale yellow	Coesite/ 183/subequant with growth structure	No cracks, strong birefringence	531.1, 10×530.9	36.2, 10×35.4/ I, 37.8/E
L003*	Copeton/ Star of the South	3/equant rounded	Pale yellow	Birefringent clinopyroxene /150/ tapered prismatic	Cracks but not reaching the surface, strong birefringence	675, 1015	22.7/E
L014	Copeton/ Star of South	2/rounded	White	Anatase granular/130/shallow oblate	Crack reaching surface, no birefringence	392.4, 514.3, 643.3	0/I
L030*	Copeton/ Deep Shaft	6/triangular rounded	White	Ca-carbonate/330, 100, 60/blebs	No cracks, no birefringence	1085	0/I
L034*	Copeton/ Streak of Luck	3/round	Pale yellow	Pale garnet/150/equant	No cracks, weak birefringence	235.1, 372.6, 549.9, 828.0, 889.1	7.6/E
L036*	Copeton/ Streak of Luck	2.5/elongate rounded	Pale yellow	Coesite/60/equant, above and touching clinopyroxene/230/ equant	No cracks, moderate birefringence	524.9/675.1	13.4/I
M14391*	Rutherglen / Great Southern Deep lead	4/round	White	Diopside/40/equant Also 400 μ equant	No cracks, moderate birefringence	669.3, 1012.9	7.6/E
M38265 VIC02	Bingara	3/rounded	Pale yellow	Coesite/150/equant grey	Cracks reaching surface, strong birefringence	532 but poorly defined	38/I
M38265 VIC6	Bingara/	4/tapered rounded	Yellow	Birefringent clinopyroxene/330/ prismatic	Cracks reaching surface, weak (shallow end) to strong birefringence (deep end)	670.9, 1016	>20/ strain birefringence
M47353	Victoria/ Eldorado	6/elongate rounded	Pale yellow	Olivine/30/equant above and in contact with 80 μ unknown, 4 nearby bladed inclusions of 80 μ size	No cracks, vague birefringence	822.7, 854.7	0/I
MR29/3	Copeton, Round Mountain	5/ elongate rounded	Yellow	Microdiamond/150/ complex of seven epitaxially joined flat triangular plates	No cracks, no birefringence	Diamond in diamond	0/I

*Means result used on Fig. 2.

However, known exceptions include (OH, F) variation in apatite and titanite, and (Al, Fe) variation in chromium spinel, so P_r determinations are most authoritative for anhydrous silicate inclusions from either the heritage or mixed group.

Assuming diamond has remained elastic, the remnant pressure (P_r) value on an inclusion generates a locus of entrapment [Eq. (2)], starting at P_r ($T=0$ °C) and extending through the diamond formation conditions (Barron, 2005):

$$P_f = (T_f^*(A_d - A_i) - P_r*B_i)/(B_d - B_i). \quad (2)$$

Using Eq. (2), formation P_f T_f space can be contoured in isobars of remnant pressure, with slopes parallel to the isovolume locus of the relevant mineral. Note that for the same value of P_r , the PPI model behaviour of two analogous mixed group minerals (i.e. adjacent in Table 3, such as garnet and clinopyroxene) will be within error of each other (see the loci for garnet – L034 and clinopyroxene – R on Fig. 2, both representing $P_r=7.6$ kbar). Heritage minerals yield inclusion entrapment loci that basically constrain the pressure of entrapment, whereas mixed group minerals primarily constrain the temperature of entrapment. Because both mixed group and heritage group minerals have generated positive remnant pressures in the Copeton diamonds, the present approach yields points of intersection between the various P_r isobars, enabling the conditions of formation to be constrained; see Fig. 2. This graphical technique is analogous to that developed by relevant researchers above, but noting that this is the first time that the various entrapment lines have high angles of intersection because the inclusions are from two different topological inclusion groups (mixed, heritage). There is an analogous resealing locus [2] for diamond that has ruptured but resealed around an inclusion.

3. Results

Twenty three diamonds with multiple inclusions and twenty nine diamonds with single inclusions were examined by Raman microprobe. Most inclusions could not be identified because there was no Raman spectral response other than from the diamond. The success rate for the technique for mineral identification is low for these rounded diamonds,

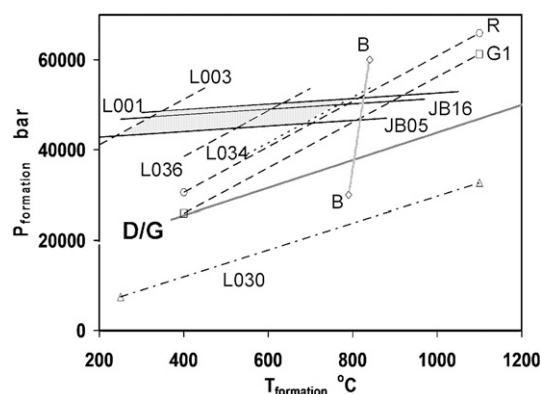


Fig. 2. Inclusion entrapment loci in PT diamond formation space for measured remnant pressure values on sealed inclusions in Copeton diamonds, relative to the diamond/graphite transition (D/G). The loci are for coesite (solid), diopside (dashed), garnet (dotted) and carbonate (dot dashed). The shaded PT region of formation of Copeton diamonds is defined by intersecting lines for stones JB05, JB16, L001, and L003, L034, L036. The B–B locus is derived from microprobe analyses of grossular diopside inclusions in Bingara diamonds and is after Davies (1998). Also shown are loci for a Mount Airly diamond (G1) and a Victorian diamond (R for Rutherglen, M14391).

with a Raman inclusion response for only 16 (6 white, 10 yellow stones) out of 52 diamonds. Probably about fifty such diamonds with inclusions should be investigated from each district in order to get a representative survey of inclusions in diamond.

Almost half of the successful inclusion identifications were from coesite under 15 to 35 kbar remnant pressure, suggesting that a high P_r may improve the response likelihood. However, several mineral inclusions close to the outer surface of the diamond with nil to low P_r were also identified, namely anatase, calcite, omphacite, and grossular garnet. The laser may not have penetrated most of the deeper inclusions in these rounded diamonds for the following four reasons: 1) Diamond surface microfeatures interfered with viewing and operating; 2) Polishing a window on the diamond might help, but may rupture the inclusion (Meyer et al., 1997; Sobolev et al., 2000), so was not attempted; 3) Some inclusions may have retracted from the inclusion chamber wall leaving behind a cavity that reflects laser light; 4) Many diamonds were fluorescent, masking the inclusion response, and sometimes triggering a secondary fluorescence in the coating on the special objectives. Changing the laser frequency may circumvent this fluorescence. Attempts to improve the likelihood of inclusion signals, using heating and cooling stages, did not succeed.

3.1. Coesite

Coesite is a heritage group inclusion. Raman spectra confirmed the presence of coesite in five Copeton diamonds (96.22, JB05, JB16, L001, L036) and one Bingara diamond (VIC02), see Table 3, all surrounded by second order birefringence in the adjacent diamond. In two of these diamonds, the inclusion chamber had ruptured with cracks reaching the surface of the diamond. The other three stones had sealed inclusion chambers without such fractures (JB05, JB16, and L001), all yellow diamonds from the Copeton district, with P_r values ranged from 31.7 to 36.2 kbar. Such values are similar to values reported by Sobolev et al. (2000) for a Venezuelan diamond and by Meyer et al. (1997; based on measurements in Milledge and Mendelsohn, 1988) for a diamond of probable African source. Most coesite inclusions in NSW diamonds are thin plates, but other identified shapes include tapered rods and equant faceted crystals. The platy coesite inclusions are likely to be the source of deep slot-like scars found penetrating many Copeton and Bingara diamonds. Fig. 3 shows the Raman spectra of various inclusions including coesite (L001), determined in-situ within the diamond.

3.2. Garnet

A garnet inclusion (mixed group) was identified in diamond L034, see Table 3. Since the inclusion was a solid solution mineral, an area scan was made over the inclusion with the main diamond peak position varying from 1330.0 cm^{-1} away from the inclusion to a maximum shift of 1332.0 cm^{-1} adjacent to the inclusion, indicating a remnant pressure of 7.6 kbar. The pale colour of this garnet, and the Raman peaks (Fig. 3), suggest it is grossular. The full width at half peak maximum of the strongest garnet peak (889 cm^{-1} , Fig. 3) is about $21 \pm 5\text{ cm}^{-1}$, and according to Gillet et al. (2002), this is within but at the uppermost limit for normally substituted garnet, but below the lower limit of 29 cm^{-1} for majoritic garnet. Davies (1998) and Davies et al. (2003) reported a composite inclusion of coesite with grossular in a diamond recovered from a Bingara deep lead.

3.3. Clinopyroxene

Clinopyroxene inclusions (mixed group) were identified from point Raman scans by comparison with Raman spectra in Wang et al. (2001), Gillet et al. (2002), and Kunz et al. (2002). Clinopyroxene is a solid solution mineral, so a Raman area scan of the host diamond was performed over the inclusion to determine the remnant pressure.

A birefringent clinopyroxene inclusion was identified in stone L003 (Table 3, see also Fig. 3). The area scan shows the main Raman spectra peak for diamond is at 1332.0 cm^{-1} away from the inclusion but has a maximum shift to 1338.0 cm^{-1} adjacent to the thickest end of the inclusion, indicating a remnant pressure of 22.7 kbar. The pyroxene Raman peaks indicate diopsidic omphacite with $\text{Mg}/(\text{Mg} + \text{Fe} + \text{Ca}) = 0.26$.

An area scan was made over an inclusion of pyroxene in Mount Airly diamond G1 (Table 3). The Raman spectra of the diamond had a peak at 1331.0 cm^{-1} away from the inclusion but shows a maximum shift to 1332.1 cm^{-1} adjacent to the inclusion, indicating a remnant pressure of 4.2 kbar. The pyroxene Raman peaks are typical of diopsidic omphacite with $\text{Mg}/(\text{Mg} + \text{Fe} + \text{Ca}) = 0.44$.

A birefringent clinopyroxene inclusion was identified in yellow Bingara diamond VIC6 (M38265, Table 3), but the inclusion chamber was ruptured with fractures reaching the surface of the stone. The adjacent diamond showed strain birefringence from second order at the still-buried deeper end of the inclusion, to weak at the shallower damaged end. The remnant pressure can be estimated as more than 20 kbar from the maximum external birefringence (Barron et al., 2008).

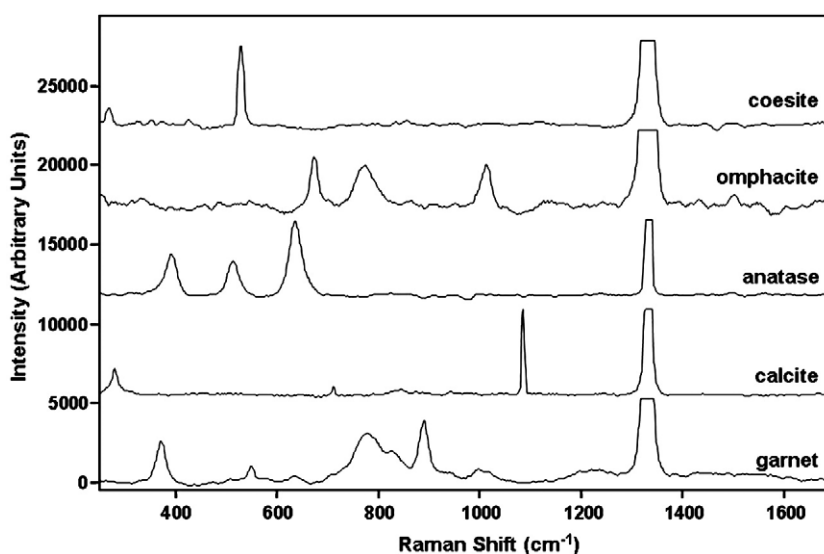


Fig. 3. Raman point spectra for inclusion in Copeton diamonds: L001 (coesite), L003 (omphacite), L014 (anatase), L030 (calcite), L034 (garnet). The broad peak at 780 cm^{-1} (garnet and omphacite charts) is due to fluorescence of the coating on the special objective used for gathering the Raman spectra.

The pyroxene Raman response indicates it is a diopsidic omphacite with $Mg/(Mg+Fe+Ca)=0.45$. This high remnant pressure on an omphacite inclusion in a Bingara diamond is similar to that found on yellow stone L003, which is an independent confirmation of a close genetic link between Bingara and Copeton diamonds. In contrast, Meyer et al. (1997; stones MR2/8, MR2B/4, MC0002/2) reported that despite aggressive polishing of large windows on three white Copeton Bingara diamonds, there was no induced-rupturing above deeply located diopside inclusions that were eventually exposed. This indicates a low remnant pressure on these inclusions, so the combined Copeton and Bingara results indicate yellow diamonds carry diopsidic omphacite inclusions under moderately high remnant pressure, whereas some white diamonds carry diopside inclusions under low remnant pressure.

The pyroxene inclusion in white Victorian diamond M14391 (Table 3) has Raman peaks indicating diopside with $X(Mg/Mg+Fe+Ca)=0.38$. The main Raman peak for unstressed diamond was at 1333.0 cm^{-1} but shifted to a maximum of 1335.0 cm^{-1} adjacent to the inclusion, equating to 7.6 kbar remnant pressure on the inclusion.

3.4. Carbonate

Most carbonates are mixed group inclusions (Barron, 2005), although those with low coefficients of thermal expansion fall in the heritage group (e.g., calcite, aragonite). Ca-carbonate was identified in three neighbouring but completely separate and sealed ovoid inclusions in L030 (Table 3), all with a main sharp peak at $1085\text{ to }1086\text{ cm}^{-1}$, and a single small sharp peak at about 750 cm^{-1} , see Fig. 3—calcite. These Raman spectral bands identify the mineral as calcite. The value for the strongest Raman peak indicates the remnant pressure on these inclusions is about 1 bar, supported by the lack of strain birefringence in the diamond around the inclusions. The inclusion chambers are unbroken but are outlined by traces of graphite on the chamber walls. Angular inclusions of Fe-calcite were identified by microprobe in four Bingara diamonds by Davies (1998), two of them nitrogen-rich stones that carry other (non-touching) inclusions with olivine (Fo_{89} , diamond B35) and omphacite-coesite (B85). Carbonate has been reported as a syngenetic inclusion in a diamond by Leung (1984) and Wang et al. (1996), and is associated with ultrahigh pressure (UHP) microdiamond inclusions in zircon (Dobrzhinestskaya et al., 2001). Davies (1998) regarded the carbonate inclusion in one of the four Bingara diamonds as secondary (diamond not specified), and secondary carbonate has been reported in Yakutian diamond (Bulanova et al., 1998).

3.5. Composite coesite–omphacite inclusion

Yellow diamond L036 (Table 3) has a small inclusion of coesite touching a larger inclusion of pyroxene. The pyroxene Raman peak indicates diopsidic omphacite with $Mg/(Mg+Fe+Ca)=0.41$. This composite inclusion confirms the coexisting association of coesite with omphacite in Copeton diamonds. The coesite spectrum corresponds to an internal pressure shift of 13.4 kbar, much lower than for the other coesite inclusions in unbroken inclusion chambers. However, the PPI model predicts this outcome because a small heritage group inclusion is in contact with a large mixed group inclusion, constraining the joint remnant pressure to be closer to the expected value of the larger inclusion (pyroxene, hence lower remnant pressure). Because the coesite inclusion has only about 2% of the volume of the touching omphacite, the coesite acts like a pressure gauge on the omphacite inclusion. As such the 13.4 kbar provides an entrapment locus for clinopyroxene (and not for coesite) on Fig. 2. Davies (1998) and Davies et al. (2003) report a Bingara diamond with non-touching coesite and omphacite inclusions.

3.6. Composite olivine inclusion

Victorian diamond M47353 (Table 3) contains a small olivine inclusion touching a mineral about 20 times larger in volume. The

Raman peaks for the olivine indicate Fo_{92} with no remnant pressure evident using the Raman curves of Keubler et al. (2005). According to the PPI model, the size contrast indicates the olivine inclusion would be responding to the completely decompressed status of the larger mineral. The latter failed to give a Raman signal so is unknown, but most likely it would be from the completely decompressed inclusion class.

3.7. Anatase

Anatase belongs to the mixed group of inclusions. Diamond L014 (Table 3) contains a shallow ovoid inclusion, with the inclusion chamber broken outward with a fracture reaching the surface. Raman peaks (Fig. 3) indicate that this inclusion is anatase with no measurable remnant pressure (and no strain birefringence in the adjacent diamond). The inclusion is cloudy with a pale dull brown colour, and is probably polycrystalline. The present form and setting of the anatase indicates it is epigenetic. Anatase has been reported as a primary inclusion in a diamond from the Finsch kimberlite pipe (Wang et al., 1996), whereas epigenetic anatase has been reported in Argyle diamond (Jaques et al., 1989).

4. Discussion and implications

4.1. Conditions of formation

The intersection of sealed-inclusion entrapment lines will indicate the diamond formation conditions, provided three conditions apply: 1) the diamonds have elastically stored (no reset) the change in PT conditions from formation to the earth's surface; 2) both heritage and mixed inclusion groups are represented in the included mineral list; and 3) the diamonds have the same provenance. Only Copeton diamonds gave results that provided such intersections (JB05, JB16, L001, L003, L034, L036, Table 3, all presumed to be high N stones due to their yellow colour), see Fig. 2. Furthermore, this response was restricted to one identified mineral in each diamond, which prevented a unique “coexisting” determination of formation conditions for a single diamond. Fig. 2 shows that the values $525\pm 275\text{ }^{\circ}\text{C}$ and $47\pm 4\text{ kbar}$ span the Copeton range of intersections. Both inclusion assemblages coesite – omphacite and coesite – grossular have been found separately in Copeton and Bingara diamond, so all intersections (Fig. 2) are equally valid. If it is assumed that these Copeton diamonds formed under one set of PT conditions, this Copeton range would have to represent the error in determining the formation conditions.

This error interpretation for the Copeton range can be refuted using the following three points: 1) Remnant pressures on sealed coesite inclusions in three stones are all within determination error ($\pm 4\text{ kbar}$) of a central value (33.5 kbar), hence the coesite entrapment loci are also within error of a central locus; 2) The Copeton range remains much larger than error despite updating in the PPI model calibration—the updated value of A_{coesite} in Table 2 is half the old value used in Barron (2005); 3) Remnant pressure values for mixed group inclusions (garnet and pyroxene) range from 7.6 to 22.7 kbar. If the inclusions were trapped under one set of PT formation conditions, the PPI model predicts that these mixed group P_r should be within error of determination ($\pm 4\text{ kbar}$). This is not the case, so the range is not within error of one set of diamond formation conditions. Is it possible that the mixed group inclusions have reset in some way, generating false P_r values?

4.2. Reset of internal pressure on inclusions in diamond

There are three identifiable styles of inclusion resets: 1) rupture with little loss of internal pressure (VIC6); 2) rupture with complete loss of internal pressure (L014); and 3) rupture and reseal under intermediate conditions (a garnet inclusion in a super-deep diamond

ruptured then resealed under cratonic diamond formation conditions; interpretation by Barron, 2005 based on data in Gillet et al., 2002). The risk of reset for any type of inclusion can be quantified using the PPI model to generate a stress history on an inclusion from the time of entrapment through to delivery of the diamond to the earth's surface. With P_d defined as the difference between confining pressure on the unruptured inclusion (internal) and confining pressure on the diamond (external), Eq. (3) is valid for any PT:

$$P_d = P_c - P = ((P - P_f) * (B_d - B_i) - (T - T_f) * (A_d - A_i)) / B_i. \quad (3)$$

PT space is contoured in P_d isobar lines parallel to the isovolume locus of the mineral, generating a P_d screen. The $P_d=0$ locus is the isobar line passing through (P_f, T_f) , whereas points at a higher P than this line yield $P_d < 0$ and those below yield $P_d > 0$. Various delivery paths were modelled using Eq. (3), which showed that actual volcanic eruption at the earth's surface represented the greatest short-term risk of diamond reset on an inclusion with P_d reaching a value between P_f and $3 \times P_f$ (depending on the temperature change) compared to $P_d = P_f$ for exhumation. Not only is P_d significantly to drastically higher for volcanic delivery, there would be explosive shocks just as P_d reached a maximum. The relative timing of actual reset can be interpreted by applying this P_d risk factor to the inclusion resets found in the present diamonds, namely early rupture plus alteration during volcanic delivery (L014, 96.22, VIC02), and late rupture after volcanic delivery (VIC6). The large Copeton range on Fig. 2 cannot be explained by any of the above three reset styles.

Is there some type of cryptic reset that interferes with the elastic behaviour of mixed group inclusions? Harris et al. (1970) suggested this after comparing two pyrope garnet inclusions with similar P_r (2; 1.7 kbar) in different African cratonic diamonds (D1; D2). These P_r values are in keeping with PPI model predictions for mixed group mineral inclusions in cratonic diamond. However, in terms of the variation of internal pressure on the inclusion with experimental heating (Table 3 in Harris et al., 1970), D1 and D2 had similar positive slopes (about 25 kbar per °C) above 450 °C, but below, the D2 slope value changed abruptly to a lower value (7.4 kbar per °C, below an internal pressure of 5 kbar). For the PPI model at constant external pressure on the diamond (1 bar), the heating slope is $dP_c/dT = (A_i - A_d) / B_i$. Although the higher Harris et al. (1970) slope value is typical of a mixed group mineral (such as garnet), the lower one is more indicative of a heritage group mineral. The overall D2 behaviour is unlike that of a simple inclusion, and topologically has the opposite behaviour of a reset/rupture. One possibility advanced by Harris et al. (D2, page 5788, 1970) was "enclosure of other material at the interface causing the pressure on the inclusion to be higher than predicted by the theory". The PPI model indicates that 1) only a heritage group mineral could cause this lower slope, and 2) since this behaviour is switched on below 5 kbar internal pressure, that heritage mineral must be supercritical fluid. It has caused a cryptic raise of about 5 kbar in the apparent P_r of D2. Such a raise is probably close to the upper limit for actual cryptic raises, because of the need to keep the mechanism hidden—requiring a small relative volume, whereas the maximum influence of fluid inclusions in diamond is given by $P_r = 16$ to 21 kbar (Navon, 1991). If a 5 kbar cryptic influence had acted on the omphacite in Copeton diamond L001, the resultant Copeton range would decrease by 110 °C, but would remain considerably larger than error. It is planned to experimentally test some of the Copeton diamonds for such cryptic influence, so it is not considered further herein.

There does not appear to be any type of resetting that can explain the large size of the Copeton temperature range. Furthermore whereas reset on a coesite inclusion (heritage group) would drop the apparent pressure of formation, reset on a pyroxene inclusion (mixed group) would tend to increase the apparent temperature of formation for any diamond (Barron, 2005). These reset directions are the opposite

required if the Copeton mixed group results (indicating UHP and low T) are due to resetting. Heritage group inclusions spontaneously generate the highest P_r (and highest maximum P_d) in diamond, so they represent the category of mineral inclusion most likely to cause chamber failure in the diamond host. The coesite inclusions in three Copeton diamonds (JB05, JB16, L001) clearly have not reset, yet they represent a potential P_d in excess of 70 kbar. If some heritage group inclusions have not reset, then reset is much less likely for mixed group inclusions (expected to have much lower P_r and P_d). Furthermore, the Copeton and Bingara inclusions/diamonds show an apparent primary variation, with compositions ranging from diopsidic omphacite (in unzoned high N yellow diamond) to diopside (in zoned low N white diamond), with P_r decreasing in that order. Thus the large size of the Copeton range is not caused by resetting or error, and hence is not consistent with a single set of diamond formation conditions.

4.3. PT conditions of Copeton diamond formation

The range of formation conditions for Copeton diamond is a primary range that must be tied to at least two sets of formation conditions: one at lower PT (250 to 500 °C, 43 to 47 kbar), and one at higher PT (800 °C, 52 kbar). These formation conditions overlap the UHP conditions of Chopin (2003), so the Copeton diamonds are UHP macrodiamonds. Eight aspects supporting this interpretation include: 1) Typical PT paths of combined subduction–exhumation are at a high angle to the Copeton diamond formation conditions, requiring more than one path to generate the Copeton range; 2) Copeton and Bingara diamonds represent a distinct type of diamond (unique inclusions, isotopic carbon is uniquely heavy, remnant pressures on mixed group inclusions are uniquely high, growth structures and mechanical defects are unique). It appears that macrodiamonds of this type have not been confirmed outside of eastern Australia; 3) Extensive post-tectonic alkali basaltic intrusions across the Bingara district have intersected at depth a Carboniferous/Mesozoic diamondiferous eclogite-dominated UHP terrane; 4) Some garnet inclusions in Bingara diamonds have a minor majoritic component, compatible with UHP conditions; 5) The chemistry of garnet and diopside inclusions in Bingara diamond yield a locus (B–B on Fig. 2) passing through UHP conditions and our estimated higher temperature set of formation conditions for Bingara–Copeton diamonds; 6) The range of compositions of pyroxene, garnet and carbonate inclusions in Copeton and Bingara diamond is similar to that reported in inclusion chambers with microdiamond in exhumed UHP terranes (Sobolev and Shatsky, 1990; Shatsky et al., 1995; Zhang et al., 1995); 7) Trace macrodiamonds have been found in exhumed UHP terranes (van Roermund et al., 2002), but are graphitized in contrast to abundant skeletal microdiamond found as inclusions trapped in porphyroblasts of garnet, pyroxene and zircon (Sobolev and Shatsky, 1990; Sobolev et al., 1994; Han et al., 1997; Massonne, 1999; Ogasawara et al., 2002; Stockhert et al., 2001; van Roermund et al., 2002; Dobrzhinestskaya et al., 2001). However, Barron (2005) showed that only the co-presence of supercritical fluid in the inclusion chambers prevented graphitization of such microdiamond; 8) Sobolev (2006) has stressed the link between coesite and continental lithosphere assemblages due to UHP metamorphism.

Combining the Copeton and Bingara evidence, the range of Copeton and Bingara diamond formation conditions indicates at least two different types of UHP protolith. The hotter material includes the incoming continental crust, whereas the colder material includes older subducted ocean plate (ocean floor sediments / basalt–gabbro / serpentinised peridotite). The higher temperature set would produce calc–silicate diamonds with inclusions of coesite, grossular, diopside, whereas the lower and middle temperature set would produce diamonds with eclogitic / peridotitic affinity (using ideas in Schulze, 1986) and inclusions of coesite–omphacite / olivine.

Six additional points need to be considered: 1) For UHP terranes, a relatively high average specific gravity would slow and stall

exhumation within the diamond stability field for considerably longer than the typical subduction/exhumation period of two million years, with the additional time spent after peak metamorphic conditions; 2) Although the low temperature end of the Copeton range might be considered remarkably low for making macrodiamond, it matches theoretical predictions for subduction diamond (200 to 600 °C, Barron et al., 1996; 350 to 650 °C, Davies, 1998; 300 to 500 °C, Griffin et al., 2000). Furthermore, Davies (1998) commented that the brittle failure during growth evident in many Bingara diamonds required anomalously low growth temperatures; 3) UHP diamond crystallisation occurs in a growth environment pervaded by high shear strain, a staccato flux of supercritical fluids, and rapidly changing pressure. This contrasts with the static conditions proposed for cratonic diamond and used for synthesis of diamond; 4) Copeton and Bingara macrodiamonds are either highly zoned (low N) or completely unzoned (high N), so there must be two new and quite different growth mechanisms for these UHP macrodiamonds, neither of which apparently applies to the abundant microdiamond (high N, trapped immediately after seed crystal formation) found typically in exhumed UHP terranes; 5) Microdiamonds are unknown in the mines of the Copeton and Bingara district, although unusual skeletal trigonal microdiamonds (0.6 to 1 mm) were recovered from modern stream sediments (Barron et al., 2005), and a trigonal microdiamond seed crystal occurs within yellow diamond MR29/3 (see Fig. 4); 6) The Copeton and Bingara UHP macrodiamonds were not graphitized, presumably because exhumation stalled within or near the diamond stability field, and the diamonds were captured by volcanic processes within 70 MY (see Introduction). However, they are significantly resorbed, a process that may have destroyed microdiamond.

4.4. Age date of Copeton and Bingara diamond

The moderate to high degree of B nitrogen aggregation found in Copeton and Bingara diamonds has been used to support an ancient origin for the diamonds (Taylor et al., 1990), but Davies (1998) and Davies et al. (2003) concluded that the strong deformation evident during growth of Bingara diamonds would greatly accelerate N-aggregation (based on Evans, 1992), and preclude an age constraint. This logic would also apply to Copeton diamonds.

Barron (2005) found that all silicate minerals typically used to age date diamond belong to the mixed group of inclusions, and their isovolume loci pass between the formation conditions of cratonic diamond and UHP diamond. Thus, these inclusions may completely decompress in cratonic diamond but retain positive P_r in UHP diamond (see Table 2). This would explain why dating of cratonic diamond using the argon trapped in a clinopyroxene inclusion tends to give the age of

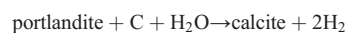
emplacement (as reported by Burgess et al., 1992). Our investigation shows that clinopyroxene inclusions in Bingara, Copeton, Mount Airly and Victorian diamonds retain elevated positive P_r (7.6 to 22.7 kbar), representing the minimum confining pressure on the inclusion regardless of delivery mechanism (Barron, 2005). Hence argon should be retained in the crystal lattice of such inclusions, so that argon isotopic age dates should be interpreted as the age of crystallisation, unless there are valid structural or isotopic reasons to the contrary. $^{40}\text{Ar}/^{39}\text{Ar}$ age dates of 340 ± 28 Ma and 326 ± 43 Ma are reported from clinopyroxene inclusions in diamonds from Copeton (Burgess et al., 1998; Pearson et al., 1998) and Bingara (Davies, 1998) respectively. As ages of crystallisation, these Carboniferous ages are within error of matching a major subduction-termination event for this part of NSW (Scheibner, 1998), and so are compatible with a local source for the alluvial diamonds via the at depth diamondiferous UHP terrane model of Barron et al. (2005, see above). A Mesozoic termination of subduction has also occurred in the region, so the analogous reasoning may apply to a Mesozoic U/Pb isotopic date reported for a mixed group titanite inclusion ($P_r > 10$ kbar, Table 2) in a Bingara diamond (Davies, 1998; Davies et al., 2002). According to Chopin (2003), all known UHP terranes have formed since the Late Proterozoic, implying the Copeton and Bingara UHP macrodiamonds are not ancient.

4.5. Other minerals reported as inclusions in Copeton and Bingara diamond

Meyer et al. (1997), Milledge et al. (1998), Davies (1998) and Davies et al. (2002, 2003) have listed silicate minerals found as syngenetic inclusions in Copeton and Bingara diamonds, see above. In addition to those found in the present research, they include melilite, scapolite, titanite and olivine, see Table 2 for the predicted responses of these minerals. In keeping with the high P_r values predicted by the PPI model, the first three are found as ruptured inclusions (Davies, 1998; Davies et al., 2003). Their reported Zr values for two titanite inclusions in a Bingara diamond result in 860–1000 °C at 50 kbar for the syngenetic inclusion and 690 °C at 1 bar for the epigenetic inclusion (using Hayden et al., 2008). These pressures were selected to fit UHP formation and volcanic delivery, and the resultant temperatures agree with this assumption. Hayden et al. (2008) show that Zr levels in titanite should increase at lower pressure, but the syngenetic titanite inclusion is isolated in diamond so it can't reset.

The proposed formation conditions show 15 to 20 kbar overpressure (pressure above the graphite diamond transition), and temperatures 250 to 700 °C too low for cratonic diamond formation. Overpressure raises the remnant pressure on inclusions in diamonds (Barron, 2005), so some negative group UHP minerals such as kyanite may occur as inclusions with low positive remnant pressure.

Calcite is a heritage group mineral (see Table 2), so the sealed carbonate inclusions in diamond L030 should generate $P_r = 23$ to 30 kbar, in contrast to the 0 kbar measured. The calcite isobar for $P_r = 0$ bar (Fig. 2) is 14 kbar below the graphite to diamond transition, indicating that calcite cannot be the original crystalline mineral trapped by this diamond. The strongest Raman spectral peak also fits aragonite and ikaite (Shahar, 2003), but they, and carbonatite melt, are also excluded, being heritage group inclusions (volume properties based on Bass, 1995; Fei, 1995; Genge et al., 1995; Pal'yanov et al., 2002; Lennie et al., 2004; Lennie, 2005). However, volumetrically these inclusions could be generated by the reaction:



(with hydrogen loss near the earth's surface driving the reaction to completion, data from Robie et al., 1979; Brown and Lamb, 1989; Brodholt and Wood, 1993). There may be more than one type of carbonate inclusion in Copeton and Bingara diamond, because some are ovoid (in L030) whereas others are angular (Davies, 1998).

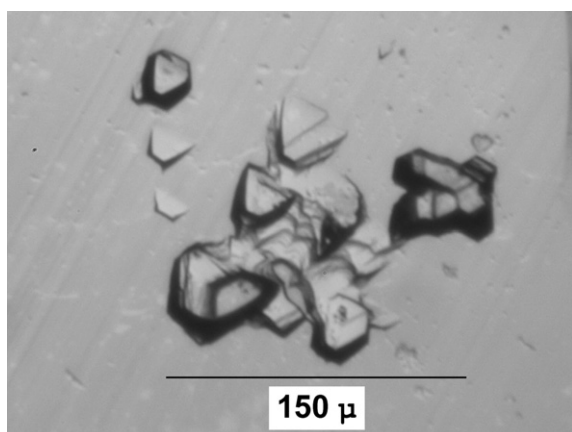


Fig. 4. Complex of trigonal microdiamond crystals as a seed in the central core of Copeton diamond MR39/3, found in diamond researched by Meyer et al. (1997).

The rupture of the anatase inclusion chamber in Copeton diamond L013 requires explanation because anatase is a mixed group inclusion, with expected low $P_f = 7 \pm 7$ kbar (Table 2, rutile would be under about 5 kbar less than this). However, at the proposed Copeton diamond formation conditions, anatase could be trapped as the high pressure polymorph (Liu and Mernagh, 1992; Sekiya et al., 2001), and the inherent 12% increase in volume due to inversion would buffer the internal pressure at 40 to 45 kbar during volcanic delivery—high enough to rupture the diamond in a shallow inclusion.

The pyroxene inclusions in diamonds from Victoria (M14391) and Mount Airly (G1) generate entrapment PT loci which are at slightly higher temperatures than the Copeton range (see Fig. 2), but are either within error or just beyond error (G1). However, both pass through reported UHP formation conditions. Relative to mixed group inclusion P_f values reported by Harris et al. (1970) for cratonic diamond, G1 is within error whereas M14391 is not. This limited data suggests the Victorian diamond is a UHP macrodiamond, but the Mount Airly diamond could be either UHP or cratonic in origin. At this time, there are no other loci to restrict the formation conditions of either Mount Airly or Victorian diamond, but coesite inclusions have been reported in Mount Airly diamonds (Sutherland et al., 1994).

5. Conclusions

Raman spectroscopic measurements on sealed inclusions in Copeton diamonds are combined with the PPI diamond-inclusion model to show that the diamonds formed over a range of 525 ± 275 °C and 47 ± 4 kbar, paralleling a primary variation in the compositions of diamonds (N) and inclusions and their remnant pressures. The Copeton and Bingara stones are macrocrystals of UHP diamond, and cannot be cratonic in origin because the formation temperatures are far too low. This generates large positive remnant pressures on minerals from the mixed group of inclusions (predicted by the PPI model, confirmed for garnet and clinopyroxene, and consistent with ruptured inclusions of titanite, melilite, anatase). The results confirm that Copeton diamond has elastically stored up the change in PT conditions from formation to delivery to the earth's surface. Values of remnant pressure are much greater than zero for clinopyroxene inclusions in Copeton, Bingara, Mount Airly and Victorian diamond, indicating that argon would remain trapped in the inclusion, so isotopic dating of such inclusions should be interpreted as the age of diamond crystallization (Carboniferous for both Copeton and Bingara diamonds).

The Copeton PT range represents at least two different sets of formation conditions derived from different protolith: 1) The lower temperature set—subducting older oceanic slab (including ocean floor sediments and mantle substrate); 2) The upper set—includes continental crust terminating subduction. This collision formed a Carboniferous/Triassic diamondiferous eclogite-dominated UHP terrane with a density high enough to allow it to stall within the diamond stability field for more than two million years. Subsequently, the terrane was decompressed by partial exhumation, trapped within the uppermost mantle and lower crust. Volcanic delivery of Copeton and Bingara diamond is implied by the presence of ruptured inclusions (common) and etched percussion marks (albeit rare), most likely by extensive post-subduction alkali basaltic magmas that definitely sampled garnet from the UHP terrane at depth. The proposed formation and delivery conditions are supported by Zr levels in syngenetic and epigenetic titanite inclusions in Bingara diamond.

Microdiamond dominates in typical exhumed UHP terranes with rare macrodiamond (graphitized). In contrast, rounded resorbed macrodiamond dominates in the Copeton and Bingara mines whereas microdiamond basically appears to be absent (probably resorbed). Although this UHP macrodiamond model holds specifically for Bingara and Copeton diamond, elsewhere in eastern Australia such diamond may be accompanied by diamond with a different origin.

Acknowledgements

The manuscript benefited from constructive reviews by L. Jaques, N. Sobolev, L. Nasdala and I. Graham. The following sources are thanked for granting access to more than 3000 diamonds from known localities: Australian Museum (Brick Clay Creek series); Cluff Resources N.L. (these Copeton and Bingara diamonds were subsequently donated to the Australian Museum collection: L and JB series, and those reported on by Meyer et al., 1997 including the MR series); Bob and Col Ribeau (Mount Airly); White Industries (Sydney, Copeton 96 and 130 series); and the Victorian Museum (M series). This manuscript is published with the permission of the Director General of the New South Wales Department of Primary Industries (Mineral Resources) and the CEO of Geoscience Australia. This publication is dedicated to my friends and colleagues Geoff Oakes and Steve Lishmund of the NSW Geological Survey, who started this research project in 1983 with controversial ideas about NSW diamond, years before I joined them!

References

- Adams, H.G., Cohen, L.H., Rosenfeld, J.L., 1975. Solid inclusion piezothermometry: II. Geometric basis, calibration for the association quartz-garnet, and application to some pelitic schists. *American Mineralogist* 60, 584–598.
- Arlt, T., Blanco, M.A., Gerward, L., Jiang, J.Z., Olsen, J.S., Recio, J.M., 2000. High pressure polymorphs of Anatase TiO₂. *Physics Review B* 61 (21), 14414–14419.
- Baker, J., 1994. Thermal expansion of scapolite. *American Mineralogist* 79, 878–884.
- Barron, L.M., 2005. A linear model and topology for the host-inclusion mineral system involving diamond. *Canadian Mineralogist* 43, 203–224.
- Barron, L.M., Lishmund, S.R., Oakes, G.M., Barron, B.J., Sutherland, F.L., 1996. Subduction model for the origin of some diamonds in the Phanerozoic of eastern New South Wales. *Australian Journal of Earth Sciences* 43, 257–267.
- Barron, B.J., Barron, L.M., Duncan, G., 2005. Eclogitic and ultra high pressure crustal garnets and their relationship to Phanerozoic subduction diamonds, Bingara area, New England Fold Belt, Eastern Australia. *Economic Geology* 100, 1565–1582.
- Barron, L.M., Mernagh, T.P., Barron, B.J., 2008. Relation between remnant pressure and strain birefringence on inclusions in diamond. *Australian Journal of Earth Sciences* 55, 159–165.
- Bass, J.D., 1995. Elasticity of minerals, glasses and melts. In: Ahrens, T.J. (Ed.), *Mineral Physics and Crystallography, Handbook of Physical Constants*. American Geophysical Union, pp. 45–63.
- Berman, R.G., 1988. Internally-consistent thermodynamic data for stoichiometric minerals in the system Na₂O–K₂O–CaO–MgO–FeO–Fe₂O₃–Al₂O₃–SiO₂–TiO₂–H₂O–CO₂. *Journal of Petrology* 29, 445–522.
- Berman, R., 1994. Density, lattice constant and expansion coefficients of diamond. In: Davies, G. (Ed.), *Properties and Growth of Diamond*. EMIS Data Reviews Series No. 9, INSPEC, The Institution of Electrical Engineers, Michael Faraday House, Stevenage, U.K., p. 23–26.
- Birch, W.D., Barron, L.M., 1997. Diamonds. In: Birch, W.D., Henry, D.A. (Eds.), *Gem minerals of Victoria*. Special Publication Mineralogical Society of Victoria, vol. 4, pp. 16–33.
- Brodholt, J., Wood, B.J., 1993. Simulations of the structure and properties of water at high pressures and temperatures. *Journal of Geophysical Research* 98, 519–536.
- Brown, P.E., Lamb, W.M., 1989. P-V-T properties of fluids in the system H₂O–CO₂–NaCl: new graphical presentations and implications for fluid inclusion studies. *Geochimica et Cosmochimica Acta* 53, 1209–1221.
- Bulanova, G.P., Griffin, W.L., Ryan, C.G., 1998. Nucleation environment of Yakutian diamond. *Mineralogical Magazine* 62, 409–419.
- Burgess, R., Turner, G., Harris, J.W., 1992. ⁴⁰Ar–³⁹Ar laser probe studies of clinopyroxene inclusions in eclogitic diamonds. *Geochimica et Cosmochimica Acta* 56, 389–402.
- Burgess, R., Phillips, D., Harris, J.W., Robinson, D.N., 1998. Antarctic diamonds in South-Eastern Australia? Hints from ⁴⁰Ar/³⁹Ar laser probe dating of clinopyroxene inclusions from Copeton diamonds. Abstracts, 7th International Kimberlite Conference, Cape Town, South Africa, pp. 119–121.
- Chopin, C., 2003. Ultrahigh-pressure metamorphism: tracing continental crust into the mantle. *Earth and Planetary Science Letters* 212, 1–14.
- Cohen, L.H., Rosenfeld, J.L., 1979. Diamond: depth of crystallisation inferred from compressed included garnet. *Journal of Geology* 87, 333–340.
- Comodi, P., Zanazzi, P.F., Poli, S., Schmidt, M.W., 1997. High-pressure behavior of kyanite: compressibility and structural deformations. *American Mineralogist* 82, 452–459.
- Davies, R.M., 1998. The characteristics and origins of alluvial diamonds from Eastern Australia. Unpublished Ph.D. thesis, Macquarie University, Sydney Australia. 209 pp. +9 appendices.
- Davies, R.M., O'Reilly, S.Y., Griffin, W.L., 2002. Multiple origins of alluvial diamonds from New South Wales, Australia. *Economic Geology* 97, 109–123.
- Davies, R.M., Griffin, W.L., O'Reilly, S.Y., Andrew, A.S., 2003. Unusual mineral inclusions and carbon isotopes of alluvial diamonds from Bingara, eastern Australia. *Lithos* 69, 51–66.
- Dobrzhiestinskaya, L.F., Green II, H.W., Mitchell, T.E., Dickerson, R.M., 2001. Metamorphic diamonds: mechanism of growth and inclusion of oxides. *Geology* 29, 263–266.

- ESPI WEB SITE, 2004. Coefficient of Thermal Expansion of Super-conductive Graphite. www.espimetals.com/tech/graphite-superconductive.pdf.
- Evans, T., 1992. Aggregation of nitrogen in diamonds. In: Field, J.E. (Ed.), *The Properties of Synthetic and Natural Diamonds*. Academic Press, pp. 259–290.
- Fedortchouk, Y., Canil, D., Carlson, J.A., 2005. Dissolution forms in Lac de Gras diamonds and their relationship to the temperature and redox state of kimberlitic magma. *Contributions to Mineralogy and Petrology* 150, 54–69.
- Fei, Y.W., 1995. Thermal expansion. In: Ahrens, T.J. (Ed.), *Mineral Physics and Crystallography. A Handbook of Physical Constants*. American Geophysical Union, pp. 29–44.
- Fei, Y., Saxena, S.K., Navrotsky, A., 1990. Internally consistent thermodynamic data and equilibrium phase relations for compounds in the system MgO–SiO₂ at high pressure and high temperature. *Journal of Geophysical Research* 95, 6915–6928.
- Genge, M.J., Jones, A.P., Price, G.D., 1995. Molecular dynamics simulations of CaCO₃ melts to mantle pressures and temperatures: implications for carbonatite magmas. *Earth and Planetary Science Letters* 131, 225–238.
- Gillet, P., Sautter, V., Harris, J., Reynard, B., Harte, B., Kunz, M., 2002. Raman spectroscopic study of garnet inclusions in diamonds from the mantle transition zone. *American Mineralogist* 87, 312–317.
- Griffin, W.L., O'Reilly, S.Y., Davies, R.M., 2000. Subduction related diamond deposits? Constraints, possibilities, and new data from Eastern Australia. *Reviews in Economic Geology* 11, 291–310.
- Han, Y.J., Zhang, Z.M., Lui, R., 1997. In: Huang, Y.H., Cao, Y.W. (Eds.), *Melt Inclusions in Eclogites from High-pressure and Ultra-high Pressure Metamorphic Belt in the Dabie Mountains, China*. Proceedings of the 30th International Geological Congress (Beijing), vol. 16. VSP, Utrecht, The Netherlands, pp. 255–263.
- Harris, J.W., Milledge, H.J., Barron, T.H.K., Munn, R.W., 1970. Thermal expansion of garnets included in diamond. *Journal of Geophysical Research* 75, 5775–5792.
- Hayden, L.A., Watson, E.B., Wark, D.A., 2008. A thermobarometer for sphene (titanite). *Contributions to Mineralogy and Petrology* 155, 529–540.
- Hazen, R.M., Finger, L.W., 1976a. The crystal structures and compressibilities of layer minerals at high pressure. II. Phlogopite and chlorite. *American Mineralogist* 63, 293–296.
- Hazen, R.M., Finger, L.W., 1976b. Crystal structures and compressibilities of pyrope and grossular to 60 kbar. *American Mineralogist* 63, 297–303.
- Helmstaedt, H., Doig, R., 1975. Eclogitic nodules from kimberlite pipes of the Colorado Plateau: samples of subducted Franciscan-type oceanic lithosphere. *Physics and Chemistry of the Earth* 9, 95–111.
- Hemley, R.J., 1987. Pressure dependence of Raman spectra of SiO₂ polymorphs: a-quartz, coesite, and stishovite. In: Manghnani, M.H., Syono, Y. (Eds.), *High-pressure Research in Mineral Physics*, Terra Scientific, Tokyo. American Geophysical Union, Washington, (D.C.), pp. 347–359.
- Holland, T.J.B., Powell, R., 1985. An internally consistent thermodynamic dataset with uncertainties and correlations: 2. Data and results. *Journal of Metamorphic Geology* 3, 343–370.
- Hollis, J.B., 2003. Morphology of diamond crystals from the Bingara Range, northern New South Wales, Australia. *Australian Gemologist* 21, 310–319.
- Horn, M., Schwertfeger, C.F., Meagher, E.P., 1972. Refinement of the structure of anatase at several temperatures. *Zeitschrift für Kristallographie* 136, 273–281.
- Izraeli, E., Harris, J.W., Navon, O., 1999. Raman barometry of diamond formation. *Earth and Planetary Science Letters* 173, 351–360.
- Jaques, A.L., Hall, A.E., Sheraton, J.D., Smith, C.B., Sun, S.-S., Drew, R.M., Foudoulis, C., Ellingsen, K., 1989. Composition of crystalline inclusions and C-isotopic composition of Argyle and Ellendale diamonds. In: Ross, J., Danchin, R.V. (Eds.), *Proceedings of the 4th International Kimberlite Conference, Kimberlites and Related Rocks—Volume 2 (IV): Their Mantle/Crust Setting, Diamonds and Diamond Exploration*. Geological Society of Australia Special Publication, vol. 14, pp. 966–989.
- Kretz, R., 1983. Symbols for rock-forming minerals. *American Mineralogist* 68, 277–279.
- Krogh, E.J., 1988. The garnet-clinopyroxene Fe–Mg geothermometer—a reinterpretation of existing experimental data. *Contributions to Mineralogy and Petrology* 99, 44–48.
- Keubler, K., Joliff, B.L., Wang, A., Hoskin, L.A., 2005. Extracting olivine (Fa–Fo) compositions from Raman spectral peak positions. Abstracts, XXXVI Lunar and Planetary Science Conference, Houston, March 2005, p. 2.
- Khokhrayakov, A.F., Pal'yanov, Y.N., 2007. The evolution of diamond morphology in the process of dissolution: experimental data. *American Mineralogist* 92, 909–917.
- Kunz, M., Gillet, P., Fiquet, G., Sautter, V., Graafsma, H., Conrad, P., Harris, J., 2002. Combined in situ X-ray diffraction and Raman spectroscopy on majoritic garnet inclusions in diamonds. *Earth and Planetary Science Letters* 198, 485–493.
- Lennie, A.R., 2005. Ikaite, (CaCO₃·6H₂O) compressibility at high water pressure: a synchrotron X-ray diffraction study. *Mineralogical Magazine* 69, 325–335.
- Lennie, A.R., Tang, C.C., Thompson, S.P., 2004. The structure and thermal expansion behaviour of Ikaite, CaCO₃·6H₂O, from T = 114 to T = 295 K. *Mineralogical Magazine* 68, 135–146.
- Leung, I.S., 1984. The discovery of calcite inclusions in natural diamond and its implications on the genesis of diamond, kimberlite and carbonatite. *Geological Society of America Abstracts with Program* 16, 574.
- Levien, L., Prewitt, C.T., 1981. High-pressure crystal structure and compressibility of coesite. *American Mineralogist* 66, 324–333.
- Liu, L.G., Mernagh, T.P., Jaques, A.L., 1990. A mineralogical Raman spectroscopy study on eclogitic garnet inclusions in diamonds from Argyle. *Contributions to Mineralogy and Petrology* 105, 156–161.
- Liu, L.G., Mernagh, T.P., 1992. Phase transitions and Raman spectra of anatase and rutile at high pressures and room temperature. *European Journal of Mineralogy* 4, 45–52.
- MacNevin, A.A., 1977. Diamonds in New South Wales. *Geological Survey of New South Wales. Mineral Resources* 42, 125 pp.
- Martens, R., Rosenhauer, M., von Gehlen, K., 1982. Compressibilities of carbonates. In: Schreyer, E. (Ed.), *High-pressure Researches in Geoscience*, Schweizerbart'sche, Stuttgart, Germany, pp. 215–222.
- Massonne, H.J., 1999. In: Gurney, J.J., Gurney, J.L., Pascoe, M.D., Richardson, S.H. (Eds.), *A New Occurrence of Microdiamonds in Quartzofeldspathic Rocks in the Saxonian Erzgebirge, Germany, and their Metamorphic Evolution*. Proceedings, 7th International Kimberlite Conference, Cape Town, South Africa, vol. 2, pp. 533–539.
- Meyer, H.O.A., Milledge, H.J., Sutherland, F.L., Kennewell, P., 1997. Unusual diamonds and unique inclusions from New South Wales, Australia. *Russian Geology and Geophysics* 38 (2), 305–331.
- Milledge, H.J., Mendelsohn, M.J., 1988. X-ray diffraction studies of coesite inclusions in diamond. *Zeitschrift für Kristallographie* 185, 609.
- Milledge, H.J., Sutherland, F.L., Kennewell, P., 1998. Further studies on Copeton diamonds. Abstracts, 7th International Kimberlite Conference, Cape Town, South Africa, pp. 587–588.
- Navon, O., 1991. High internal pressures in diamond fluid inclusions determined by infrared-absorption. *Nature* 353, 746–748.
- Ogasawara, Y., Ohta, M., Fukasawa, K., Katayama, I., Maruyama, S., 2002. Diamond-bearing and diamond-free metacarbonate rocks from Kumdy-Kol in the Kokchetav massif, northern Kazakhstan. *Island Arc* 9, 400–416.
- Olinger, B., 1977. Compression studies of forsterite, Mg₂SiO₄ and enstatite, MgSiO₃. In: Manghnani, M.H., Akimoto, S.I. (Eds.), *High Pressure Research Applications in Geophysics*. Academic Press, New York, pp. 325–334.
- O'Reilly, S.Y., 1989. Nature of the east Australia lithosphere. In: Johnson, R.W. (Ed.), *Intraplate Volcanism in Eastern Australia and New Zealand*. Cambridge University Press, Cambridge, U.K., pp. 290–297.
- Pal'yanov, Y.N., Sokol, A.G., Borzdov, Y.M., Khotkhrayakov, A.F., Sobolev, N., 2002. Diamond formation through carbonate-silicate interaction. *American Mineralogist* 87, 1009–1013.
- Pearson, D.G., Davies, R.M., Shirey, S.B., Carlson, R.W., Griffin, W.L., 1998. The age and origin of eastern Australian diamonds: Re/Os isotope evidence from sulfide inclusions in two diamonds from Wellington, New South Wales. Extended Abstracts, 7th International Kimberlite Conference, Cape Town, South Africa, pp. 664–666.
- Reeder, R.J., Markgraf, S.A., 1986. High temperature crystal chemistry of dolomite. *American Mineralogist* 71, 705–804.
- Robie, R.A., Hemingway, B.S., Fisher, J.R., 1979. Thermodynamic properties of minerals and related substances at 298.15 K and 1 bar, 105 pascals pressure and at higher temperatures. *United States Geological Survey Bulletin* 1452 456 pp.
- Robinson, D.N., 1978. The characteristics of natural diamond and their interpretation. *Minerals Science Engineering* 10, 55–72.
- Robinson, D.N., 1980. Surface textures and other features of diamonds. Unpublished Ph. D. thesis, University of Cape Town, Rondebosch, South Africa, 221 pp.
- Robinson, D.N., Scott, J.A., van Niekerk, A., Anderson, V.G., 1989. The sequence of events reflected in the diamonds of some southern African kimberlites. In: Ross, J., Danchin, R.V. (Eds.), *Proceedings of the 4th International Kimberlite Conference, Kimberlites and Related Rocks, Their Mantle/Crust Setting 2(IV)*. Geological Society of Australia Special Publication, vol. 14, pp. 990–1000.
- Rosenfeld, J.L., Chase, A.B., 1961. Pressure and temperature of crystallization from elastic effects around solid inclusions in minerals. *American Journal of Science* 259, 519–541.
- Scheibner, E., 1998. *Geology of New South Wales—Synthesis: v. 2 Geological Evolution*. Department of Mineral Resources, Geological Survey NSW Memoir Geology, vol. 13. 2. 666 pp.
- Schulze, D.J., 1986. Calcium anomalies in the mantle and a subducted metaserpentinite origin for diamonds. *Nature* 319, 483–484.
- Sekiya, T., Ohta, S.S., Kurita, S.S., 2001. Optical properties of anatase TiO₂ under high pressure. *International Journal of Modern Physics B* 15, 3952–3955.
- Shahar, A., 2003. The stability of Ikaite, CaCO₃·6H₂O, at high pressure and temperature. Abstract, Geological Society America. Annual Meeting, Seattle, USA, November 2–5, Paper, vol. 259–8.
- Shatsky, V.S., Sobolev, N.V., Vavilov, M.A., 1995. Diamond-bearing metamorphic rocks of the Kokchetav massif (North Kazakhstan). In: Coleman, R.G., Wang, X.M. (Eds.), *Ultrahigh Pressure Metamorphism*. Cambridge University Press, pp. 427–455.
- Smith, F.G., 1953. *Historical Development of Inclusion Thermometry*. Toronto. University of Toronto Press, Toronto, Canada. 149 pp.
- Sobolev, N.V., 1984. Crystalline inclusions in diamonds from New South Wales, Australia. In: Glover, J.E., Harris, P.G. (Eds.), *Kimberlite Occurrence and Origin, A Basis for Conceptual Models in Exploration*. University of Western Australia, Publication, vol. 8, pp. 213–226.
- Sobolev, N.V., 2006. Coesite as an indicator of ultrahigh pressure in continental lithosphere. *Russian Geology and Geophysics* 47, 95–104.
- Sobolev, N.V., Shatsky, V.S., 1990. Diamond inclusions in garnets from metamorphic rocks: a new environment for diamond formation. *Nature* 343, 742–746.
- Sobolev, N.V., Shatsky, V.S., Vavilov, M.A., Goryainov, S.V., 1994. Zircon of high pressure metamorphic rocks of folded areas as unique container of inclusions of diamond, coesite and coexisting minerals. *Doklady Akademii Nauk* 354, 488–492.
- Sobolev, N.V., Fursenko, B.A., Goryainov, S.V., Shu, J.F., Hemley, R.J., Mao, H.K., Boyd, F.R., 2000. Fossilized high pressure from the Earth's deep interior: the coesite–in-diamond barometer. *Proceedings of the National Academy of Sciences of the United States of America* 97 (22), 1875–1879.
- Spear, F.S., 1993. *Metamorphic Phase-equilibria and Pressure–Temperature–Time Paths*. Monograph, vol. 1. Mineralogical Society of America, Washington, D.C. 799 pp.
- Stockhert, B., Duyster, J., Trefmann, C., Massonne, H.J., 2001. Microdiamond daughter crystals precipitated from supercritical CO₂+silicate fluids included in garnet, Erzgebirge, Germany. *Geology* 29, 391–394.
- Sueno, S.M., Cameron, M., Papke, J.J., Prewitt, C.T., 1973. The high temperature crystal chemistry of tremolite. *American Mineralogist* 61, 38–53.

- Sutherland, F.L., Barron, L.M., 2003. Diamonds of multiple origins from New South Wales: further data and discussion. *Australian Journal of Earth Sciences* 50, 975–981.
- Sutherland, F.L., Hollis, J.D., Raynor, L.R., 1985. Diamonds from nepheline mugarite? A discussion of 'Garnet websterites' and associated ultramafic inclusions from a nepheline mugarite in the Walcha area, New South Wales, Australia. *Mineralogical Magazine* 49, 748–751.
- Sutherland, F.L., Temby, P., Raynor, L.R., Hollis, J.D., 1994. A review of the East Australian Diamond Province. In: Meyer, H.O.A., Leonardos, O.H. (Eds.), *Diamonds II: Characterisation, Genesis and Exploration*. International Kimberlite Conference, 5th, Araxa, Brazil, Proceedings, pp. 170–184.
- Tang, J., Qin, L.C., Sasaki, T.Z., Yudasaka, M.S., Matsushita, A.Y., Iijima, S.M., 2000. Compressibility and polygonization of single-walled carbon nanotubes under hydrostatic pressure. *Physical Review Letters* 85, 1887–1889.
- Tardieu, A., Cansell, F., Petit, J.P., 1990. Pressure and temperature dependence of the first-order Raman mode of diamond. *Journal of Applied Physics* 68, 3243–3245.
- Taylor, W.R., Jaques, A.L., Ridd, M., 1990. Nitrogen-defect aggregation characteristics of some Australasian diamonds: time-temperature constraints on the source regions of pipe and alluvial diamonds. *American Mineralogist* 75, 1290–1310.
- van Roermund, H.L.M., Carswell, D.A., Drury, M.R., Heijboer, T.C., 2002. Microdiamonds in a megacrystic garnet websterite pod from Bardane on the island of Fjortoft, western Norway: evidence for diamond formation in mantle rocks during deep continental subduction. *Geology* 30, 959–962.
- Wang, A., Pasteris, J.D., Meyer, H.O.A., Dele-Duboi, M.L., 1996. Magnesite-bearing inclusion assemblage in natural diamond. *Earth and Planetary Science Letters* 141, 293–306.
- Wang, A., Jolliff, B.L., Haskin, L.A., Kuebler, K.E., Viskupic, K.M., 2001. Characterisation and comparison of structural and compositional features of planetary quadrilateral pyroxenes by Raman spectroscopy. *American Mineralogist* 86, 790–806.
- Wechsler, B.A., Prewitt, C.T., 1984. Crystal structure of ilmenite (FeTiO₃) at high temperature and high pressure. *American Mineralogist* 69, 176–185.
- Xu, S.T., Liu, Y.C., Chen, G.B., Wu, W.P., 2005. Architecture and kinematics of the Dabie Orogen, Central Eastern China. *Acta Geologica Sinica* 79, 356–371.
- Zhang, Y.X., 1998. Mechanical and phase equilibria in inclusion-host systems. *Earth and Planetary Science Letters* 157, 209–222.
- Zhang, J.Z., Reeder, R.J., 1999. Comparative compressibility of Calcite-structure carbonates: deviations from empirical relations. *American Mineralogist* 84, 861–870.
- Zhang, R.Y., Liou, J.G., Ernst, W.G., 1995. Ultrahigh-pressure metamorphism and decompressional P–T paths of eclogites and country rocks from Weihai, eastern China. *Island Arc* 4, 293–309.